Interface Focus

FirstCite® e-publishing

Interface Focus
doi:10.1098/rsfs.2011.0093
Published online

Kaleidoscopic tilings, networks and hierarchical structures in blends of 3-miktoarm star terpolymers

Jacob Judas Kain Kirkensgaard*

Department of Basic Sciences and Environment, Faculty of Life Sciences, University of Copenhagen, Denmark

Dissipative particle dynamics simulations are used to explore blends of 3-miktoarm star terpolymers. The investigated system is a 50/50 blend of ABC and ABD stars, which is investigated as a function of composition and at different symmetric segregation levels. The study shows that in analogy to pure ABC star melts cylindrical tiling patters form, but now in four-coloured variants. Also, a large part of the phase diagram is dominated by multi-coloured network structures showing hierarchical features. Most prominently, a novel alternating gyroid network structure with a hyperbolic lamellar interface is predicted to form. Here, the two gyroidal nets are composed of respectively C and D components, with the minority A and B components forming the lamellar-like curved structure on the dividing interface between the two nets.

Keywords: soft matter; self-assembly; miktoarm star copolymers

1. INTRODUCTION

Block copolymers, macromolecules with two or more different homopolymer chains covalently bound at junction points, remain a subject of intense research interest owing to the tunable physical properties and the many possible nanostructures obtainable both controllably and reproducibly [1,2]. These properties originate from the tendency of the various polymer chains to undergo phase separation, which is allowed only to a certain degree owing to the inherent constraint of the molecular connectivity between the different polymer blocks. In generic terms, the simplest block copolymer system is an AB diblock copolymer where two polymer chains A and B are joined at a single junction point (figure 1*a*). Diblock copolymers have been the subject of interest for many years and their self-assembly is generally well understood [4]. The structural phase behaviour of AB diblock copolymers is usually mapped out as a function of two parameters: the composition, i.e. the relative volume fractions of the two components, and the degree of segregation described by the product χN with χ being the Flory–Huggins segment–segment interaction parameter and N the degree of polymerization [5,6]. A characteristic feature of diblock copolymer self-assembly is that as the segregation becomes stronger, the phase behaviour becomes completely dominated by the composition. As a function of the composition described by the A component volume fraction f_A ($f_B = 1 - f_A$), the universal phase diagram in the strong segregation limit consists of four ordered mesostructures, namely lamellar, bicontinuous gyroid, hexagonally arranged cylinders and a body-centred cubic sphere packing in principle appearing symmetrically around a 50/50 composition when assuming complete chemical symmetry between the two components. The addition of a third component markedly increases the morphological phase space as seen with linear ABC terpolymers where a wealth of different structures have been found [1]. A unifying feature between these structures and those found in AB systems is that they are all characterized by the *interfaces* of each pair of polymer species. However, another option when adding a third component is to create a star-like topology instead of a linear chain, thus creating a so-called *ABC miktoarm star terpolymer* (figure 1*b*). The self-assembly behaviour of ABC 3-miktoarm star terpolymers have been investigated both experimentally [7] as well as by simulations [3,8,9] and field theory [10,11]. The generic theoretical phase diagram as mapped out by these sources is shown in figure 1*c* under the constraint of symmetric interaction parameters between the different polymer species and the compositional constraint of two components occupying equal volume fractions. Despite these severe constraints, a fundamental result appears compared with the self-assembly of linear block copolymers: the molecular star topology dictates the formation of ABC lines where the three different interfaces between AB, AC and BC meet [3,12]. As a consequence, a sequence of cylindrical structures following various polygonal tiling patterns appears. This sequence of tilings has been predicted from all the earlier mentioned theoretical studies and has been found in a number of experimental ABC 3-miktoarm star terpolymer systems [13–15].

*kirkensgaard@life.ku.dk

One contribution to a Theme Issue 'Geometry of interfaces: topological complexity in biology and materials'.

Received 4 October 2011
Accepted 15 December 2011

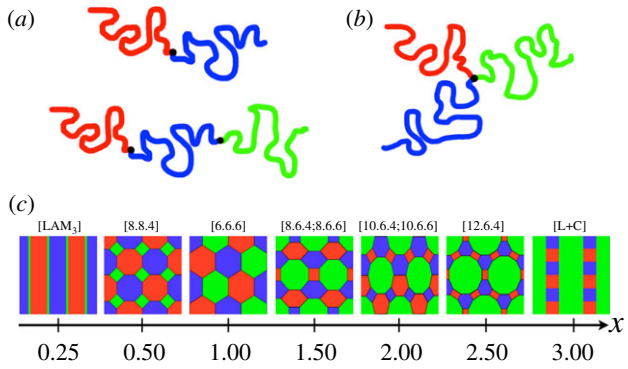

Figure 1. (*a*) Linear AB diblock copolymer and ABC triblock terpolymer. (*b*) ABC 3-miktoarm star terpolymer. (*c*) Schematic phase diagram for ABC 3-miktoarm star terpolymers under the constraint of the A and B components occupying equal volume fractions and invoking symmetric interactions between all unlike components. The different phases are placed at their approximate compositional positions quantified by the parameter x, the volume ratio of the C and A components. Colour code: A, red; B, blue; C, green. The different tilings are named by their Schläfli symbol [3], a set of numbers $[k_1.k_2 \ldots .k_l]$ indicating that a vertex is surrounded by a k_1-gon, a k_2-gon, ... in cyclic order. Tilings with more than one topologically distinct vertex are denoted $[k_1.k_2.k_3; k_4.k_5.k_6]$.

Recently, experimental results showing interesting new morphologies are emerging involving blends of ABC 3-miktoarm star terpolymers with other polymer species. For example, blending an ABC star that alone forms the [6.6.6] tiling pattern with C homopolymer chains leads to a zinc-blende structure with alternating AB domains building up a diamond network [16]. Also, blending an ABC star that forms the [12.6.4] tiling alone with AB diblock copolymers can cause the A and B components to swap polygonal symmetry positions in the tiling pattern [17]. Thus, blending opens up the possibility of tuning the structures found in the pure systems or allowing completely new morphologies to appear. Here, we show how blending two different miktoarm stars allows the formation of a range of new multi-coloured structures. The possible phase space of a blend of different miktoarm stars is gigantic. The variables in play are (i) the molecular topology, i.e. the connectivity of the chains, (ii) the composition, i.e. the number and relative sizes or volume fractions of the different chains including the blend ratio, and (iii) the chemical nature of the constituent polymer species, i.e. their mutual interaction parameters. Here, we constrain the investigation to looking at a 50/50 mixture of ABC and ABD 3-miktoarm stars (figure 2). Also, the A and B chains are constrained to have equal size as are the pair of C and D chains. The lengths of these two pairs are then varied relative to each other. Thus, we can quantify the compositional phase behaviour in this very restricted investigation by the x parameter mentioned earlier in the caption to figure 2 defined as the volume fraction ratio of the C component to the A component. This means we can directly compare our results with the generic phase progression seen in pure ABC 3-miktoarm star terpolymer melts shown above in figure 1*c*.

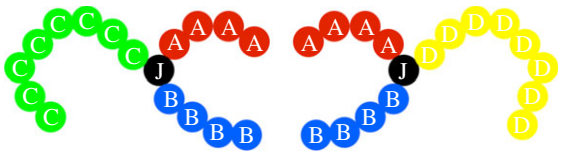

Figure 2. Model ABC and ABD 3-miktoarm stars investigated in this paper. A central junction bead connects three chains. The red A and blue B chains are constrained to have equal size in both molecules. The green C and yellow D chain lengths are also constrained to have the same size, but this is varied relative to the length of the A and B chains. The composition is quantified by the parameter x, here equal to $8/4 = 2$ (the number ratio of C to A beads) or by the C component volume fraction $f_C = 8/16 = 0.5$ in this example (excluding the junction bead).

2. SIMULATION SET-UP

The self-assembly of the miktoarm stars is explored using dissipative particle dynamics (DPD) simulations following the implementation described previously [18]. Specific details about employed parameters are as follows: the interactions between any two different polymer species i and j separated by a distance r_{ij} are described by the soft potential

$$V_{\text{soft}}(r_{ij}) = \begin{cases} \dfrac{a_{ij}}{2}\left(1 - \dfrac{r_{ij}}{r_c}\right)^2 & \text{for } r_{ij} \le r_c \\ 0 & \text{for } r_{ij} > r_c, \end{cases} \tag{2.1}$$

with $r_c = 1$ and beads are connected with harmonic bonds via the potential

$$V_{\text{bond}} = \frac{C}{2}(r_{ij} - r_0)^2, \tag{2.2}$$

with $r_0 = 0$ and $C = 4$. The integration of the equations of motion is done using a standard velocity–Verlet algorithm with time step $\Delta t = 0.02$ and $k_B T = 1$. All simulations are performed in a cubic box of volume L^3 and with particle density $\rho = 3$. For all structures different box sizes have been checked to eliminate finite size effects [18]. At a density of $\rho = 3$, the interaction parameter between unlike particles can be related to the Flory–Huggins interaction parameter χ_{ij} [19] so that

$$a_{ij} = a_{ii} + 3.497\chi_{ij}, \tag{2.3}$$

with the like–like interaction parameter determined from the compressibility of water to be $a_{ii} = 25$ [19]. Here, we take a purely qualitative approach exploring generic traits and do not intend to match any specific polymer system. We assume symmetric cross interaction between all unlike polymer species and investigate different segregation levels with $a_{ij} = 36$, 40, 60 and 80, respectively. The only exception to this is the single junction bead in each molecule which is set to be neutral and acts as a like particle to all species. Simulations were run using the ESPResSo package [20] within the framework developed earlier to simulate branched molecules in general [21]. Simulation snapsnots were all made with the Visual Molecular Dynamics (VMD) package [22].

3. RESULTS

In figure 3, a phase diagram is shown as a function of composition and symmetric interaction strength. The composition is described either by the combined volume fraction of the C and D components or alternatively by the parameter x defined earlier. We will use the latter in the following. At $x = 0.28$, the morphology is a lamellar structure as expected, only now it is a four-coloured version when compared with the regular ABC 3-miktoarm star lamellar structure found at corresponding values of x. However, we should expect the equilibrium structure to be one with fully segregated domains arranged as ACBDACBDA, but this is not what is predicted from the simulations. At low segregation, the minority components simply mix and the resulting lamellae is similar to that found in regular ABC star systems, i.e. an [LAM_3] morphology as shown in figure 1*c*. It is not macrophase separated as shown in figure 4*a* where we see a single simulation box with several lamellae periods. At higher segregation, the morphology is a hierarchical structure with the two majority components forming lamellae in one direction and the two minority components forming a layer in between showing lamellar ordering in the perpendicular direction. We denote this [$LAM_{CD\text{-}in\text{-}AB}$] (figure 4*b*). Within the timescales investigated here, the expected equilibrium structure mentioned earlier has not been found. Probably, there is a window where the predicted [$LAM_{CD\text{-}in\text{-}AB}$] structure is at least metastable because the segregation strength between the two minority components is low. In the [$LAM_{CD\text{-}in\text{-}AB}$] morphology, both of the long chains are comfortably positioned in their own domains; so one has to flip one of those chains (plus the minority component itself) all the way through a layer of the other majority species to form the pure ACBDACBDA arrangement. Since N is higher for the majority components, the energetic cost for this to happen is larger than the gain of separating the two minority components, thus making the formation of the four-coloured lamellae prohibitively difficult.

A similar thing occurs at the highest x value investigated, $x = 14$. Here, the variation of the interaction parameters from low to high leads to a phase progression going from macrophase-separated ABC and ABD stars, through another network structure (discussed below) to lamellar structures, first with the minority components mixed at the C–D interface like the $[LAM]_3$ structure and then segregated at the interface similar to the previously discussed structure (figure 4*c*). Thus, as is the case with the phase progression of ABC 3-miktoarm stars shown above in figure 1*c*, the limits of the phase diagram is composed of lamellar structures. As noticed by a referee, it is counterintuitive to find macrophase-separated structures at low segregation strength and then microphase separation at higher segregation. However, this stems from a subtle interplay between composition and the increased number of interaction parameters (greater than 2). If we consider for a second the minority A–B part (and junction) to be a single component we call M, the system is in principle a blend of M-b-C and M-b-D diblocks at this high value of x. Hamley and co-workers

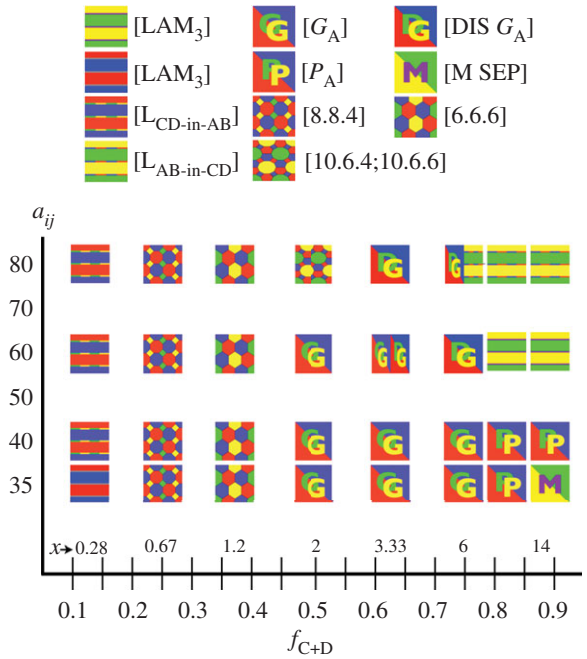

Figure 3. Phase diagram of a blend of ABC and ABD 3-miktoarm star terpolymers as a function of composition and interaction strength. The x parameter is indicated in the figure. Note that at some points in the phase diagram, two different phases were stabilized several times. These are indicated by half-sized icons.

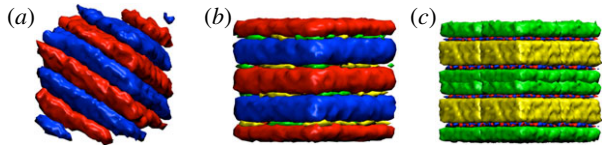

Figure 4. Lamellar structures found at the boundaries of the investigated phase diagram. (*a*) [LAM_3] structure found at $x = 0.28$ with $a_{ij} = 36$. (*b*) [$LAM_{CD\text{-}in\text{-}AB}$] at $x = 0.28$ with $a_{ij} = 80$. (*c*) [$LAM_{AB\text{-}in\text{-}CD}$] at $x = 14$ with $a_{ij} = 80$. (*a*,*b*) show single box views, (*c*) shows $2 \times 2 \times 2$ boxes.

[23] investigated blends of poly(styrene)–poly(isoprene) and poly(isoprene)–poly(ethylene oxide), and found the same behaviour experimentally as well as predicted theoretically using the random phase approximation: upon increasing interaction parameter, the system goes from a disordered state (not seen in these simulations, but would appear at lower a_{ij}) to a macrophase-separated state and finally to a microphase-separated state. Similar conclusions have also been drawn elsewhere [24], along with predictions of additional interesting possibilities such as critical phenomena, all stemming from such competition between micro- and macro-phase separation.

At $x = 0.67$, we enter a region with a progression of tiling patterns, also in four-coloured variants. We find that for all segregation levels, the system adopts the [8.8.4] and [6.6.6] tilings for $x = 0.67$ and $x = 1.2$, respectively. At $x = 2$, we find the [10.6.4;10.6.6] tiling, but only at high segregation, $a_{ij} = 80$. The compositional positioning of the underlying tiling patterns are in complete agreement with the progression found in normal ABC star systems shown in figure 1*c*, i.e. a [8.8.4] tiling at $x \sim 0.5$, a [6.6.6] tiling at $x \sim 1$ and a

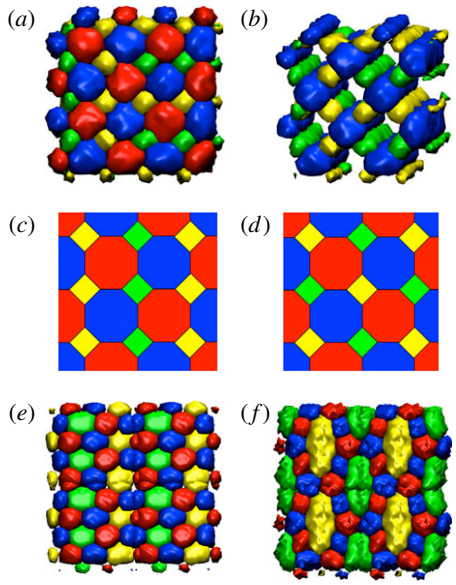

Figure 5. Kaleidoscopic tiling patterns found in this study. (*a*) [8.8.4], (*b*) same as (*a*) but tilted and omitting the red A component. Note that there are defects along the cylinder axis in the minority component domains. (*c*,*d*) Two different but equally favourable four-colourings of the [8.8.4] tiling. (*e*) [6.6.6] and (*f*) [10.6.4;10.6.6]. (*e*,*f*) Are $2 \times 2 \times 2$ simulation boxes.

[10.6.4;10.6.6] tiling at $x \sim 2$. The three four-coloured tiling patterns are shown in figure 5. For the [8.8.4] tiling, we show two alternative arrangements of the minority components C and D which we consider the most probable equilibrium structures (figure 5*c*,*d*). However, it has not been possible to stabilize either of these two patterns uniquely at $x = 0.67$. The underlying tiling is always [8.8.4], but there are usually defects along the cylinder axis in the form of colour swapping between the C and D components (figure 5*b*), or defects where the same patterns appear to form in perpendicular directions. The latter can be seen in figure 5*a*, where two such domains meet along a boundary passing down through the central vertical row of red/blue domains. The majority components A and B always form fully segregated cylindrical domains. Defects in the minority components along the symmetry axis are also occasionally seen with the other two tilings found, but to a much lesser degree.

In all of the earlier cited simulation investigations of ABC 3-miktoarm stars done in three-dimensional space, branched structures have been found for $2 < x < 3$, but so far no particular ordered structure has been assigned in this composition region. This it not the case here. Our simulations predict a large composition range where ordered networks are formed. First, as seen in figure 3, a novel network structure with hierarchical features form for $x = 2 - 6$ and $a_{ij} \leq 60$. In this structure, the two majority components C and D each form a chiral **srs**-net, one left- and one right-handed, separated by a membrane following a gyroid surface ('**srs**' follows the Reticular Chemistry Structure Resource naming convention [25]). On this surface, the two minority components A and B form a curved lamellar pattern. Thus, this structure is an alternating gyroid

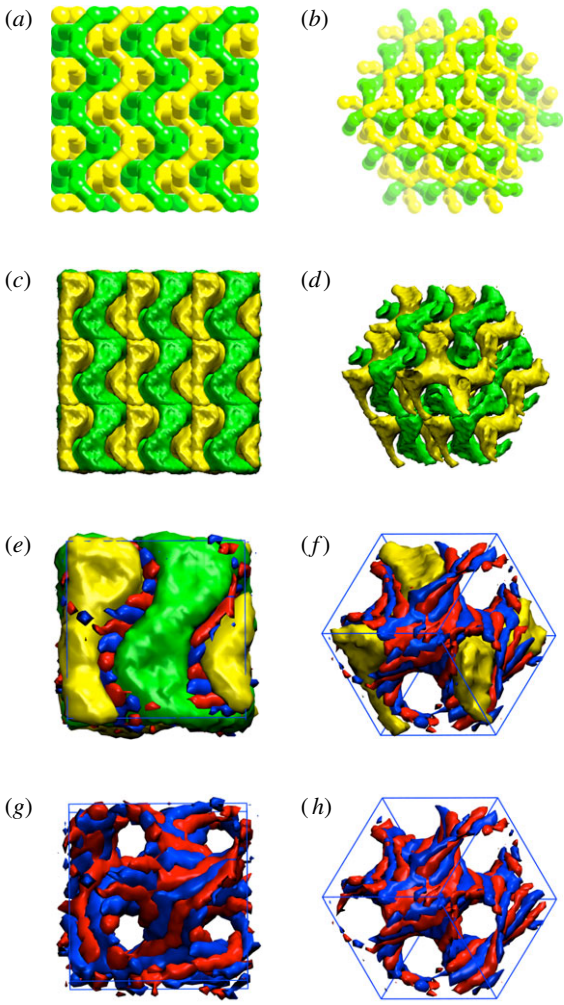

Figure 6. Alternating gyroid with hyperbolic lamellar interface [G_A]. Left column show views along the [100] direction and right column along [111]. (*a*,*b*) Crystallographic models of two intertwined **srs**-nets. (*c*,*d*) Simulation snapshots of $3 \times 3 \times 3$ boxes matching (*a*,*b*). (*e*)–(*h*) Single box views illustrating the AB hyperbolic lamellae membrane separating the two nets.

with a hyperbolic lamellar interface. We denote the structure [G_A] and illustrate it in more detail in figure 6. We believe this is the first prediction of this particular structure. Alternating gyroids have been predicted and found in linear ABC terpolymer systems though [26]. In those, the A and C components each form an srs-net separated by a matrix of the B component. A notable difference here is that the nets now constitute the majority of the composition in contrast to regular AB diblock and linear ABC gyroids, where the networks are minority components in a matrix of something else. However, a related structure has been described recently in a ABC 3-miktoarm star system not subject to the constraints invoked in the simulations here of equal A and B volumes and symmetric interactions [7]. Here, the system is roughly a 1 : 2 : 3 ABC star where the majority C component forms a regular gyroid structure (i.e. the C component builds up both nets), which is separated by a hyperbolic surface with the A and B components segregated. However, in that particular system, the interaction parameters are far from symmetric and quite large between

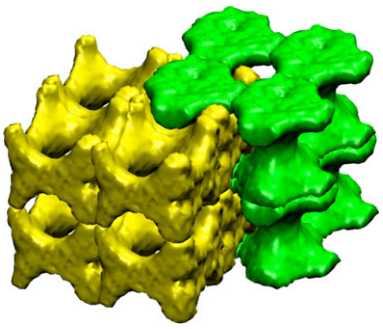

Figure 7. Alternating P [P_A] composed of two intertwined six-connected **pcu**-nets predicted in a small window in the phase diagram. The A, B and junction components form a curved interface separating the two nets (not shown). Each colour represents 2×2 simulation boxes.

the two minority components leading to the formation of a gyroid film consisting of globular A domains wrapped by the B component.

At $x = 3.33$ and $x = 6$ and $a_{ij} \geq 60$, the simulations predict a morphology that has similarities with the alternating gyroid and also appears to be a three-coordinated net. Like the gyroid structure it is composed of two continuous domains of C and D separated by a surface of segregated A and B again forming a hyperbolic lamellar pattern. We believe that this is most likely an artefact from the cubic box and that upon suitable adjustment of the box shape, the predicted morphology would here also be the alternating gyroid. We denote these points in the phase diagram with [DIS G_A], for distorted gyroid.

As mentioned already, at low segregation strength but high x we find another two-coloured network structure denoted [P_A], this morphology being an analogue to the bicontinuous P structure also found in many soft matter systems (figure 7). Again, the two majority components each forms a net, here a six-coordinated cubic **pcu**-net; the nets are mutually intertwined and separated by a thin layer of the minority components that, in this case, does not form any ordered structure. We note that the formation of the P structure has been predicted computationally in simpler linear systems of AB diblocks [27] and ABC triblocks [28] blended with homopolymers; however, these have not been confirmed experimentally [26].

To summarize, we have shown that blending different miktoarm stars potentially allows the formation of new complex kaleidoscopic multi-component morphologies. It is particularly interesting that a significant part of the phase diagram mapped out here consists of network structures that are usually only found in a less dominant degree. However, it is already known that multiple continuous network structures persist over broader compositional ranges in linear ABC terpolymers compared with AB diblocks [26]. Thus, it is not as such surprising that the increased interfacial interactions originating from the multi-component nature of these systems would act to stabilize more complex structures as seen here. We await future experimental investigations to clarify if these remarkable structures can be found in real systems.

Thanks to Kell Mortensen and the referees for useful comments to the manuscript. Parts of this research was undertaken on the NCI National Facility in Canberra, Australia, which is supported by the Australian Commonwealth Government. Financial support from The Lundbeck Foundation and UNIK Synthetic Biology is gratefully acknowledged.

REFERENCES

1 Hadjichristidis, N., Iatrou, H., Pitsikalis, M., Pispas, S. & Avgeropoulos, A. 2005 Linear and non-linear triblock terpolymers. synthesis, self-assembly in selective solvents and in bulk. *Prog. Polym. Sci.* **30**, 725–782. (doi:10.1016/j.progpolymsci.2005.04.001)

2 Abetz, V. & Simon, P. F. W. 2005 Phase behaviour and morphologies of block copolymers. *Adv. Polym. Sci.* **189**, 125–212. (doi:10.1007/12_004)

3 Gemma, T., Hatano, A. & Dotera, T. 2002 Monte Carlo simulations of the morphology of ABC star polymers using the diagonal bond method. *Macromolecules* **35**, 3225–3227. (doi:10.1021/ma001040q)

4 Matsen, M. W. & Schick, M. 1994 Stable and unstable phases of a diblock copolymer melt. *Phys. Rev. Lett.* **72**, 2660–2663. (doi:10.1103/PhysRevLett.72.2660)

5 Huggins, M. 1941 Solutions of long chain compounds. *J. Chem. Phys.* **9**, 440. (doi:10.1063/1.1750930)

6 Flory, P. 1942 Thermodynamics of high polymer solutions. *J. Chem. Phys.* **10**, 51. (doi:10.1063/1.1723621)

7 Matsushita, Y., Hayashida, K., Dotera, T. & Takano, A. 2011 Kaleidoscopic morphologies from ABC star-shaped terpolymers. *J. Phys. Condens. Matter* **23**, 284111. (doi:10.1088/0953-8984/23/28/284111)

8 Huang, C.-I., Fang, H.-K. & Lin, C.-H. 2008 Morphological transition behavior of ABC star copolymers by varying the interaction parameters. *Phys. Rev. E* **77**, 031804. (doi:10.1103/PhysRevE.77.031804)

9 Kirkensgaard, J. J. K. 2011 Systematic progressions of core-shell polygon containing tiling patterns in melts of 2nd generation dendritic miktoarm star copolymers. *Soft Matter* **7**, 10 756–10 762. (doi:10.1039/C1SM06115A)

10 Zhang, G., Qiu, F., Zhang, H., Yang, Y. & Shi, A. 2010 SCFT study of tiling patterns in ABC star terpolymers. *Macromolecules* **43**, 2981–2989. (doi:10.1021/ma902735t)

11 Li, W., Xu, Y., Zhang, G., Qiu, F., Yang, Y. & Shi, A. 2010 Real-space self-consistent mean-field theory study of ABC star triblock copolymers. *J. Chem. Phys.* **133**, 064904. (doi:10.1063/1.3469857)

12 Sioula, S., Hadjichristidis, N. & Thomas, E. 1998 Direct evidence for confinement of junctions to lines in an 3-miktoarm star terpolymer microdomain structure. *Macromolecules* **31**, 8429–8432. (doi:10.1021/ma980622t)

13 Takano, A. *et al.* 2004 Observation of cylinder-based microphase-separated structures from ABC star-shaped terpolymers investigated by electron computerized tomography. *Macromolecules* **37**, 9941–9946. (doi:10.1021/ma048893t)

14 Takano, A. *et al.* 2007 Composition dependence of nanophase-separated structures formed by star-shaped terpolymers of the $A_{1.0}B_{1.0}C_x$ type. *J. Polym. Sci. B Polym. Phys.* **45**, 2277–2283. (doi:10.1002/polb.21241)

15 Hayashida, K., Kawashima, W., Takano, A., Shinohara, Y., Amemiya, Y., Nozue, Y. & Matsushita, Y. 2006 Archimedean tiling patterns of ABC star-shaped terpolymers studied by microbeam small-angle X-ray scattering. *Macromolecules* **39**, 4869–4872. (doi:10.1021/ma060647p)

16 Hayashida, K., Takano, A., Dotera, T. & Matsushita, Y. 2008 Giant zincblende structures formed by an ABC

star-shaped terpolymer/homopolymer blend system. *Macromolecules* **41**, 6269–6271. (doi:10.1021/ma801367v)
17 Abetz, V. & Jiang, S. 2004 Formation of superlattices in blends of 3-miktoarm star terpolymers with diblock copolymers. *e-Polymers* **54**, 1–9.
18 Kirkensgaard, J. J. K. 2010 Novel network morphologies and compositionally robust 3-colored perforated lamellar phase in $A(BC)_2$ miktoarm star copolymer melts. *Soft Matter* **6**, 6102–6108. (doi:10.1039/c0sm00358a)
19 Groot, R. & Warren, P. 1997 Dissipative particle dynamics: bridging the gap between atomistic and mesoscopic simulation. *J. Chem. Phys.* **107**, 4423. (doi:10.1063/1.474784)
20 Limbach, H. J., Arnold, A., Mann, B. A. & Holm, C. 2006 Espresso: an extensible simulation package for research on soft matter systems. *Comp. Phys. Comm.* **174**, 704–727. (doi:10.1016/j.cpc.2005.10.005)
21 Kirkensgaard, J. J. K. & Hyde, S. 2009 Beyond amphiphiles: coarse-grained simulations of star-polyphile liquid crystalline assemblies. *Phys. Chem. Chem. Phys.* **11**, 2016–2022. (doi:10.1039/b818032f)
22 Humphrey, W., Dalke, A. & Schulten, K. 1996 VMD: visual molecular dynamics. *J. Mol. Graph.* **14**, 33–38. (doi:10.1016/0263-7855(96)00018-5)
23 Frielinghaus, H. *et al.* 2001 Micro- vs. macro-phase separation in binary blends of poly(styrene)-poly(isoprene) and poly(isoprene)-poly(ethylene oxide) diblock copolymers. *Europhys. Lett.* **53**, 680–686. (doi:10.1209/epl/i2001-00205-7)
24 Olmsted, P. & Hamley, I. 1999 Lifshitz points in blends of AB and BC diblock copolymers. *Europhys. Lett.* **45**, 83. (doi:10.1209/epl/i1999-00135-4)
25 O'Keeffe, M., Peskov, M., Ramsden, S. & Yaghi, O. 2008 The reticular chemistry structure resource (RCSR) database of, and symbols for, crystal nets. *Acc. Chem. Res.* **41**, 1782–1789. (doi:10.1021/ar800124u)
26 Meuler, A., Hillmyer, M. & Bates, F. 2009 Ordered network mesostructures in block polymer materials. *Macromolecules*, **42**, 7221–7250. (doi:10.1021/ma9009593)
27 Martinez-Veracoechea, F. & Escobedo, F. 2009 Bicontinuous phases in diblock copolymer/homopolymer blends: simulation and self-consistent field theory. *Macromolecules* **42**, 1775–1784. (doi:10.1021/ma802427a)
28 Dotera, T. 2002 Tricontinuous cubic structures in ABC/A/C copolymer and homopolymer blends *Phys. Rev. Lett.* **89**, 205502. (doi:10.1103/PhysRevLett.89.205502)